4D GPR Fluid Flow Visualization in Fractured Carbonates at the 1 to 10 m Scale*

Mark Grasmueck[1], Pierpaolo Marchesini[1], Gregor P. Eberli[1], Michael Zeller[1], and Remke L. Van Dam[2]

Search and Discovery Article #120056 (2013)
Posted January 22, 2013

*Adapted from extended abstract prepared in conjunction with poster presentation at AAPG Hedberg Conference, Fundamental Controls on Flow in Carbonates, July 8-13, 2012, Saint-Cyr Sur Mer, Provence, France, AAPG©2012

[1]Center for Carbonate Research, University of Miami, FL, USA (pmarchesini@rsmas.miami.edu)
[2]Department of Geological Sciences, Michigan State University, East Lansing, MI, USA

Abstract

Three thousand liters of water were infiltrated from a 4 m diameter pond to track flow and transport inside fractured carbonates with 20-40% porosity. Sixteen time-lapse 3D Ground Penetrating Radar (GPR) surveys with repetition intervals between 2 hours and 5 days monitored the spreading of the water bulb in the subsurface. Based on local travel time shifts between repeated GPR survey pairs, localized changes of volumetric water content can be related to the processes of wetting, saturation and drainage. Deformation bands consisting of thin subvertical sheets of crushed grains reduce the magnitude of water content changes but enhance flow in sheet parallel direction. This causes an earlier break through across a stratigraphic boundary compared to porous limestone without deformation bands. This experiment shows how 4D GPR can non-invasively track ongoing flow processes in rock-volumes of over 100 m3.

Introduction and Significance

Time-lapse 3D GPR is the repeated acquisition of identical surveys to track dynamic processes in the near surface. As water content is the main factor controlling the propagation of electromagnetic waves in geologic materials, 4D GPR can be used to image and quantify flow and transport in unsaturated domains. Such non-invasive flow characterization at the 1 to 10 m scale helps in upscaling permeability and porosity measurements obtained from small rock plugs.

The objective of this work is to extract local time shifts between precisely repeated high-resolution 3D GPR surveys for detection of water content changes in three dimensions. The goal is to relate the GPR time shifts to zones of wetting, saturation and drainage in fractured rock. The field site for the experiment is a fractured high-porosity limestone exposed in a quarry. The following paragraphs give more detailed descriptions of the quarry location and geology, design of the infiltration experiment, and the GPR system used for rapid and precise data acquisition. The results show to our knowledge for the first time a 3D snapshot of ongoing water bulb propagation during a 3 hour time window and how flow is affected by fractures and stratigraphy.

Field Site Description

The Madonna della Mazza quarry located in central Italy (Figure 1a) is cut into a succession of rudist-derived grain stones of upper Cretaceous age. The porosity ranges from 20-40%. The quarry is 64 m long (east-west), and 50 m wide (north-south) with walls rising to a maximum height of 12 m. The ground water table in the quarry is well below the GPR investigation depth. The stratigraphy in the quarry is rather uniform and bedding dips gently to the NE. The bedding surfaces are often represented by thin fine-grained layers. The outcropping wall and floor of the quarry have been studied in detail (Tondi et al, 2006). The fracture network consists of faults and deformation bands. Faults are open fractures with displacement. Deformation bands are defined by typically 0.2-0.5 cm thick subvertical sheets of crushed grains and compaction without an open fracture. The hydrological character of deformation bands and faults is opposite: Deformation bands often produce a reduction in permeability and porosity, whereas open fractures cause a permeability increase.

The 4D GPR Monitored Infiltration Experiment

With the aid of a 3D GPR survey acquired in the previous field season the 4 m diameter infiltration pond area was positioned to include a portion of intact porous limestone, a zone with a cluster of deformation bands, and part of a fault (Figure 1b). The open fracture of the fault was sealed at the surface with cement to prevent direct entry of water from the pond.

A first pair of dry 3D GPR 200 MHz surveys was acquired to image the pre-infiltration condition. The line spacing was 0.05 m. Each 20x20 m GPR survey consisting of 401 profiles took between 105-180 minutes to acquire depending on the walking speed of the operator (Figure 2). The 8 m wide rim between pond wall and 3D GPR survey edge allows lateral movement of the infiltrated water and is also necessary for the 3D migration aperture, especially at larger depths.

After completion of the pre-infiltration 3D GPR survey pair, the plastic pond wall was sealed to the quarry floor. The pond was filled with a 9 cm water head at the lowest point. Once the water level dropped to 8 cm, water was added to reach the 9 cm head again.

Infiltration of 1 cm water head took about 1.5 hours. This procedure was followed to approximate a constant head in the pond. After 30 hours the infiltration of 3000 liters of water was completed. As soon as there was no more standing water, the pond walls were removed and the first post-infiltration GPR survey was acquired. We continued to record a total of seven 3D GPR survey pairs over the next 5 days. We gradually increased the interval between the GPR surveys as water movement slows down due to the expansion of the water bulb.

Data Processing and Warp Time Shift Extraction

The sixteen 3D GPR surveys are processed with identical steps and parameters: Data fusion, gridding, dewow (7 ns window), time zero correction, gain application, background removal, and 3D migration. The gained data are 3D phaseshift migrated in Promax with a constant velocity of 0.09 m/ns. Experience has shown that even for the 3D surveys acquired during the infiltration experiment this dry velocity still adequately reduces the diffractions so the subsequent warping mostly correlates reflection events. The warping step extracts the 3D volume of vertical time shifts necessary to match two repeat 3D GPR surveys to each other. The 4D Warp routines in Promax originally developed for 4D seismic processing, correlate small 3D subvolumes and compute the optimum vertical time shift necessary to match up corresponding GPR events.

Results

Survey Nomenclature

The pre-infiltration surveys are numbered DRY1 and DRY2, according to the sequence of acquisition. The fourteen post-infiltration surveys are labeled with the time after the start of the infiltration. As no surveys could be recorded during the 30 hour infiltration due to the pond wall and standing water, the first post-infiltration survey is labeled with WET32hr meaning that the acquisition of the survey started 32 hours after the start of the infiltration. It took two hours to remove the pond wall and setup the 3D GPR system before the first data trace was acquired.

Repeatability

For the ideal case of perfectly repeatable 3D GPR surveys, subtraction of data volumes should highlight only the incremental changes due to dynamic processes and suppress the stationary geological structures. To benchmark repeatability of our surveying and processing technique we acquired two “identical” surveys just before the injection experiment began. As seen in Figure 3 for sample Inline 186 extracted from the center of the 3D survey, the subtraction of the two migrated pre-injection surveys contains random noise and remains of very low amplitude geological reflections. Exceptions are a dipping shallow event and parts of the first break at the

very top of the profile. These signals do not cancel out during subtraction. The cause can be either a difference in the survey track or the signal amplitudes are clipped in one of the repeat surveys by exceeding the 16 bit dynamic range of the GPR analog to digital converter.

Comparison of Post-Infiltration 3D GPR Surveys and Time Shift Visualization

The comparison of pre-infiltration survey (Figure 3a) with first post-infiltration survey (Figure 4a) shows pronounced amplitude changes and time shifts. The visual differences between the WET32hr and WET35hr post-infiltration survey pair are subtle. However the warp time shifts between these two surveys show a coherent negative anomaly below the infiltration pond (Label A in Figure 4c). The core of the anomaly has a -1.2 ns maximum shift. The pull-up is caused by the saturated water bulb sinking deeper and draining the rock volume above the bulb. The time shifts outside the influence of the pond infiltration can be used to determine the noise level of the time shift data volume. Here, time shifts are positive and negative and absolute values are below 0.2 ns. These random time shifts can be caused by slight deviations in data acquisition from the ideal survey grid, migration processing noise and warp uncertainty. In order to better visualize the time shift anomaly caused by water content changes, time shift values $\geq$ (-0.2) ns are set completely transparent in Figure 5. The stepped colorbar creates contours helpful in visualizing gradients within the time shift data. The reason for this is that time shift gradients are a direct indicator of local water content changes (Truss et al, 2007).

Interpretation of the Time Shift Data

The WET32hrΔWET35hr time shift volume provides a snapshot of the changes in the water bulb which occurred in the 3 hour interval between the two time-lapse surveys. Over this short period the total amount of water within the survey volume did not change assuming evaporation is negligible. Therefore the positive (water content increases) and negative gradients (water content decreases) are balanced producing closed shape anomalies. The time shift anomaly in Figure 5 is closed but strongly asymmetric both in terms of extent and gradients. Comparing the opposite sides (see also labels R, S, P, and Q on Figure 5) of the anomaly yields some interesting insights about the ongoing water bulb propagation processes:

- The vertical extension of the infiltration time shift anomaly defined by the -0.6 ns contour is more than double at label R compared to S. The core of the anomaly with time shifts larger than -0.6 ns is relatively flat indicating no change in water content. This is the center of the water bulb which is always saturated during the 3 hour observation period. The saturated zone is better developed in the porous host rock (R) than in (S) where deformation bands are present. The upper slope of the anomaly is the drain zone as the water bulb sinks deeper. The slope on underside of the anomaly represents the wetting front, the transition from initially dry condition to fully saturated.

- Time shifts along vertical column P have steeper gradients and reach a higher maximum than in column Q. The higher the maximum time shift the higher the total amount of water content change. More water is therefore moving in the porous limestone without deformation bands. However the vertical extension of the entire time shift anomaly measured inside the -0.2 ns contour is larger for Q than for P. Apparently the deformation bands facilitate wider spreading of water but the local water content changes are smaller. The deformation bands also help transport water across the stratigraphic boundary. In P the water bulb has not yet entered the deeper layer. In the porous limestone without deformation bands the thin fine grained bedding surface presents a flow barrier at this stage of the infiltration experiment. Here the wetting bulb anomaly is confined by this stratigraphic boundary.

Discussion and Conclusion

Direct verification of time-lapse GPR results in rocks is difficult due to lack of accessibility to the subsurface for direct observation of flow processes. However the excellent exposure of strata and fractures in the Madonna della Mazza quarry allows indirect verification and reasoning. After the completion of the infiltration, the porous limestone between the deformation bands stayed damp for several hours similar to wicks transporting moisture by capillary force to the exposed rock surface. On the other hand, the deformation bands dried up in the sun within minutes, confirming their low hydraulic conductivity. Based on these outcrop observations and sample analyses, deformation bands are thin subvertical sheets with reduced hydraulic conductivity due to grain crushing and compaction. It is therefore no surprise that the extent and gradients of the time shift anomaly caused by the propagation of the wetting bulb are strongly influenced by the presence of deformation bands. The GPR time-lapse data show how they reduce the time shift gradients and therefore the local water content changes. At the same time the deformation bands cause a faster and wider spreading of the wetting bulb and facilitate transport across a stratigraphic boundary.

These preliminary results are encouraging but the 16 time-lapse 3D GPR volumes recorded during the experiment still contain a wealth of information that has yet to be exploited. For example, the role of the fault intersecting the infiltration pond at the southern boundary is not clearly defined in the WET32hr and WET35hr survey pair. However a total of 105 combinations of pairs of repeated surveys can be used to calculate local time shifts and track flow with time increments between 2 hours and several days. The practical problem is that time-lapse 3D GPR processing is computationally very demanding and the average time for a full-density warp calculation of one survey pair is 8 days on a single core 3GHz CPU.

Once the local time shifts within high-resolution 3D GPR time-lapse surveys can be efficiently and reliably extracted, the next step will be to apply petrophysical transfer functions such as the Topp equation or a Mixing Model (Robinson et al., 2003) to compute fields of in situ water content change and water bulb mass balances.

Acknowledgments

This research is supported by the Sponsors of the Comparative Sedimentology Laboratory at the University of Miami and the National Science Foundation (Grant No. 0323213 and No. 0440322). The University of Miami acknowledges the support of this research by Landmark Graphics Corporation via the Landmark University Software Grant Program.

References Cited

Grasmueck, M., and D.A. Viggiano, 2007, Integration of Ground-Penetrating Radar and Laser Position Sensors for Real-Time 3D Data Fusion: IEEE Transactions on Geoscience and Remote Sensing, v. 45/1, p. 130-137.

Robinson, D.A., S.B. Jones, J.M. Wraith, D. Or, and S.P. Friedman, 2003, A review of advances in dielectric and electrical conductivity measurements in soils using time domain reflectometry: Vadose Zone J., v. 2, p. 444-475.

Tondi, E., M. Antonellini, A. Aydin, L. Marchegiani, and G. Cello, 2006, The role of deformation bands, stylolites and sheared stylolites in fault development in carbonate grainstones of Majella Mountain, Italy: Journal of Structural Geology, v. 28, p. 376-391.

Truss S., M. Grasmueck, S. Vega, and D.A. Viggiano, 2007, Imaging rainfall drainage within the Miami oolithic limestone using high-resolution time-lapse ground-penetrating-radar: Water Resources Research, v. 43:W03405, doi:10.1029/2005WR004395.

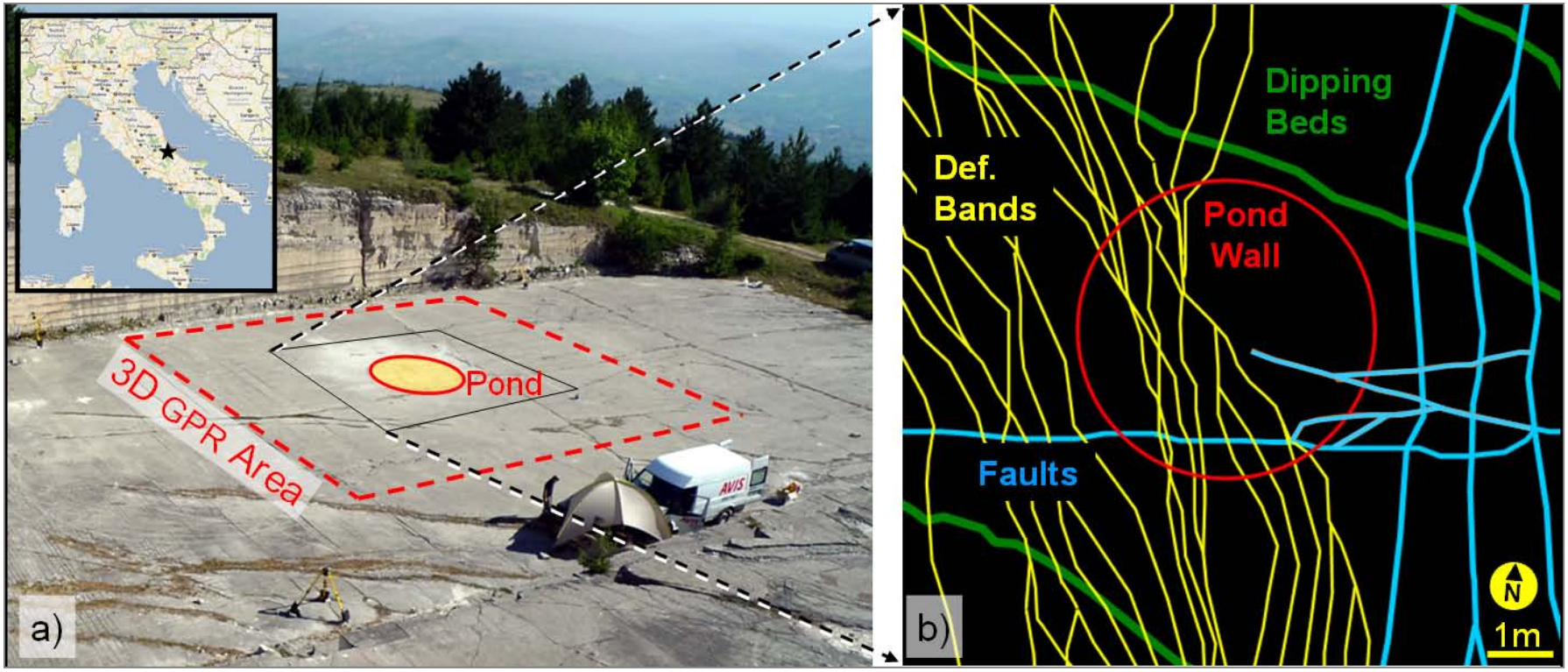

Figure 1. Overview of the Madonna della Mazza quarry located near the village of Pretoro in central Italy. (a) A temporary infiltration pond was installed on the quarry floor at the center of the 20x20 m 3D GPR time-lapse survey area. (b) Map view of pond location with structural and geological interpretation based on quarry floor observations and shallow horizontal slices extracted from 3D GPR data.

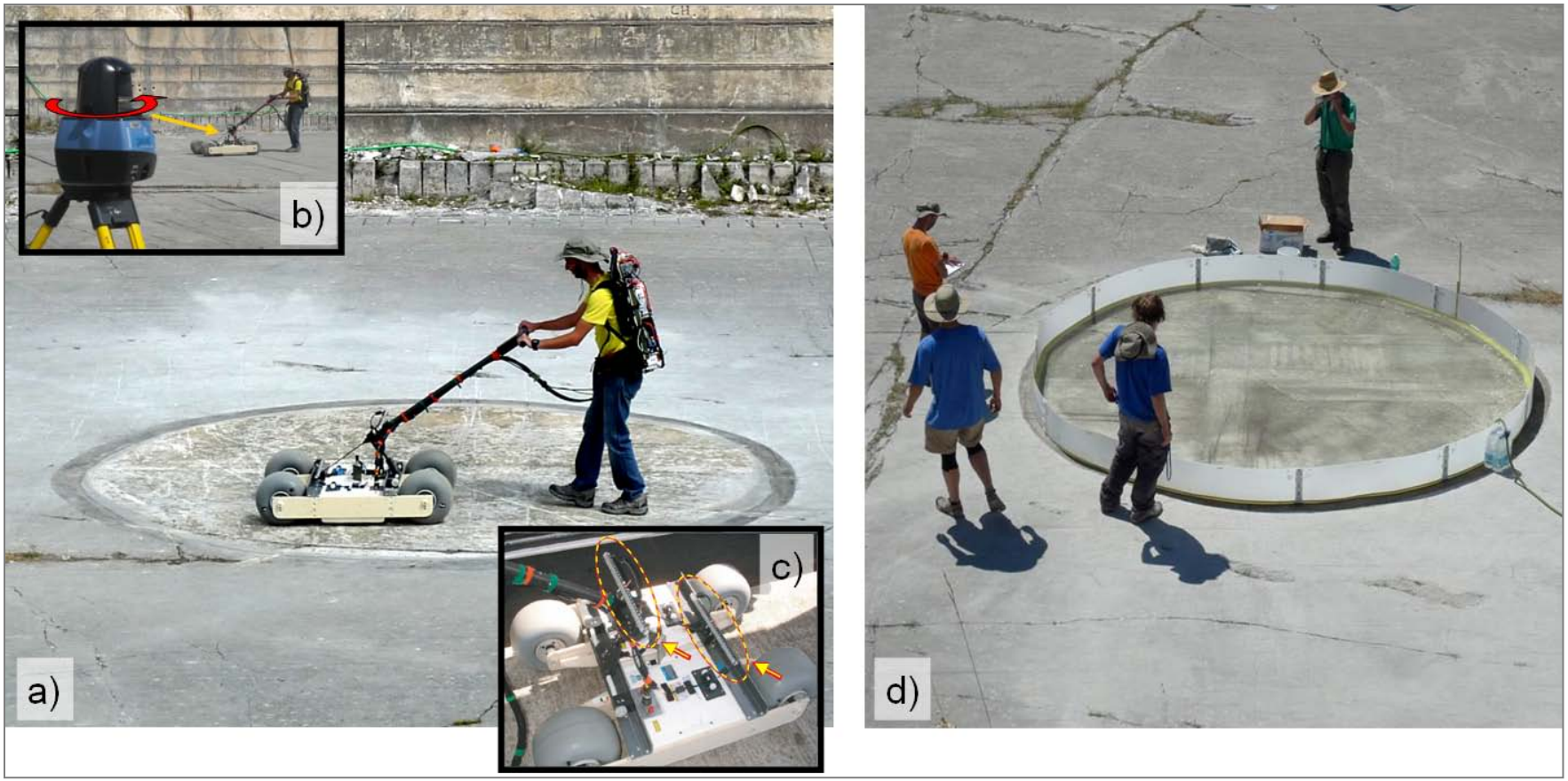

Figure 2. (a) Acquisition of the 20x20 m 3D GPR survey with dual 200 MHz antenna cart and 0.05 m line spacing. (b) Centimeter precise positioning was achieved with a Rotary Laser Positioning System (Grasmueck and Viggiano, 2007) consisting of 4 spinning laser beacons transmitting infrared and laser pulses to a small detector mounted in the center of the GPR cart. (c) With 20 position updates per second the operator of the cart is guided in real-time by two linear LED arrays along the profile lines. Average walking speed is 1 m/s. (d) The 4 m diameter infiltration pond was filled with a maximum of 9 cm of water.

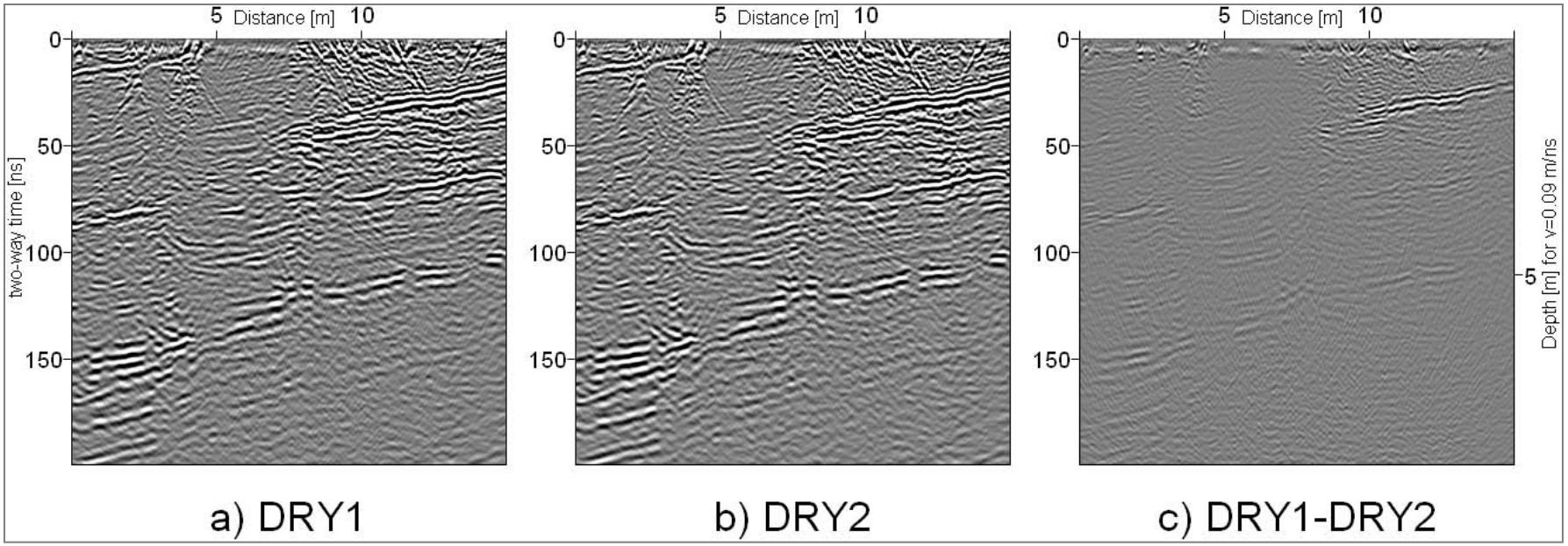

Figure 3. Inline 186 extracted from the center of the 3D migrated DRY cubes. (a, b) For quality control of survey repeatability two pre-infilration 3D GPR surveys where acquired. (c) Subtraction of the two DRY surveys produces low random noise and cancels most geological reflections. Exceptions are a shallow dipping strong amplitude event and parts of the first break arrivals exceeding the 16 bit dynamic range of the A/D converter. Display gain is identical for all 3 panels.

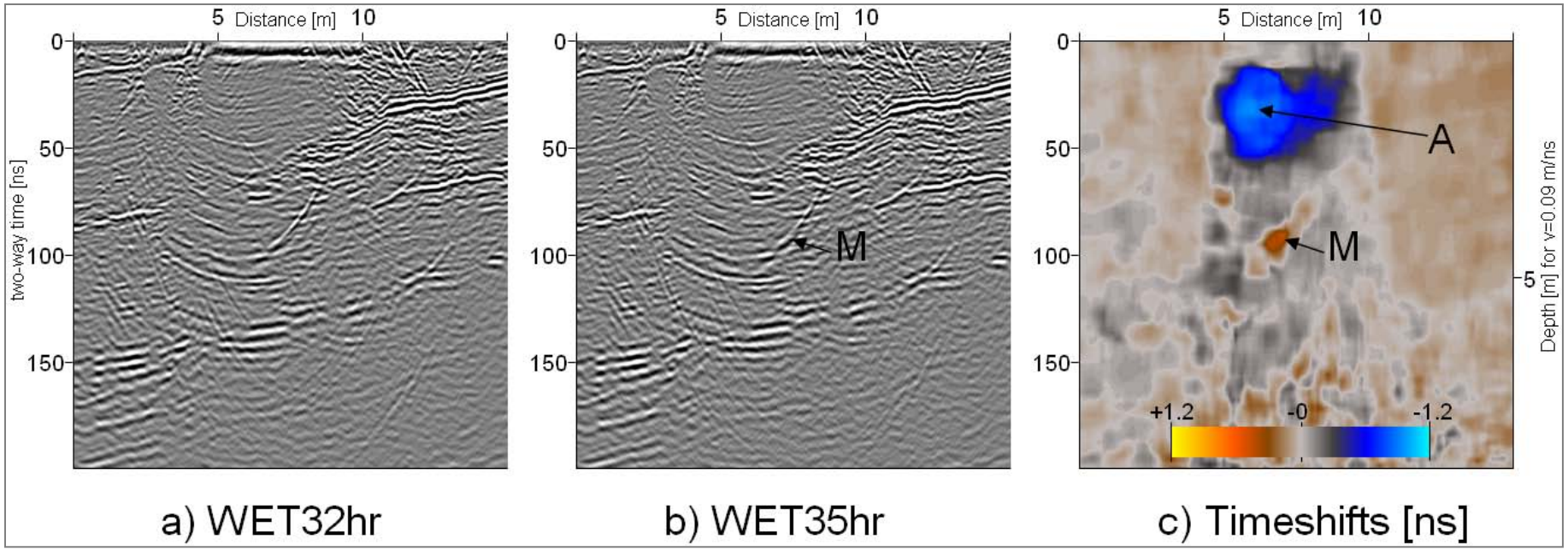

Figure 4. Inline 186 extracted from the center of the 3D migrated WET cubes. (a, b) Comparison of the first 2 repeat surveys acquired just after completion of the infiltration. (c) The local time shifts WET32hrΔWET35hr extracted with warp processing show a strong negative anomaly (labeled A) below the infiltration area. Label M denotes a positive time shift anomaly caused by a migration artifact.

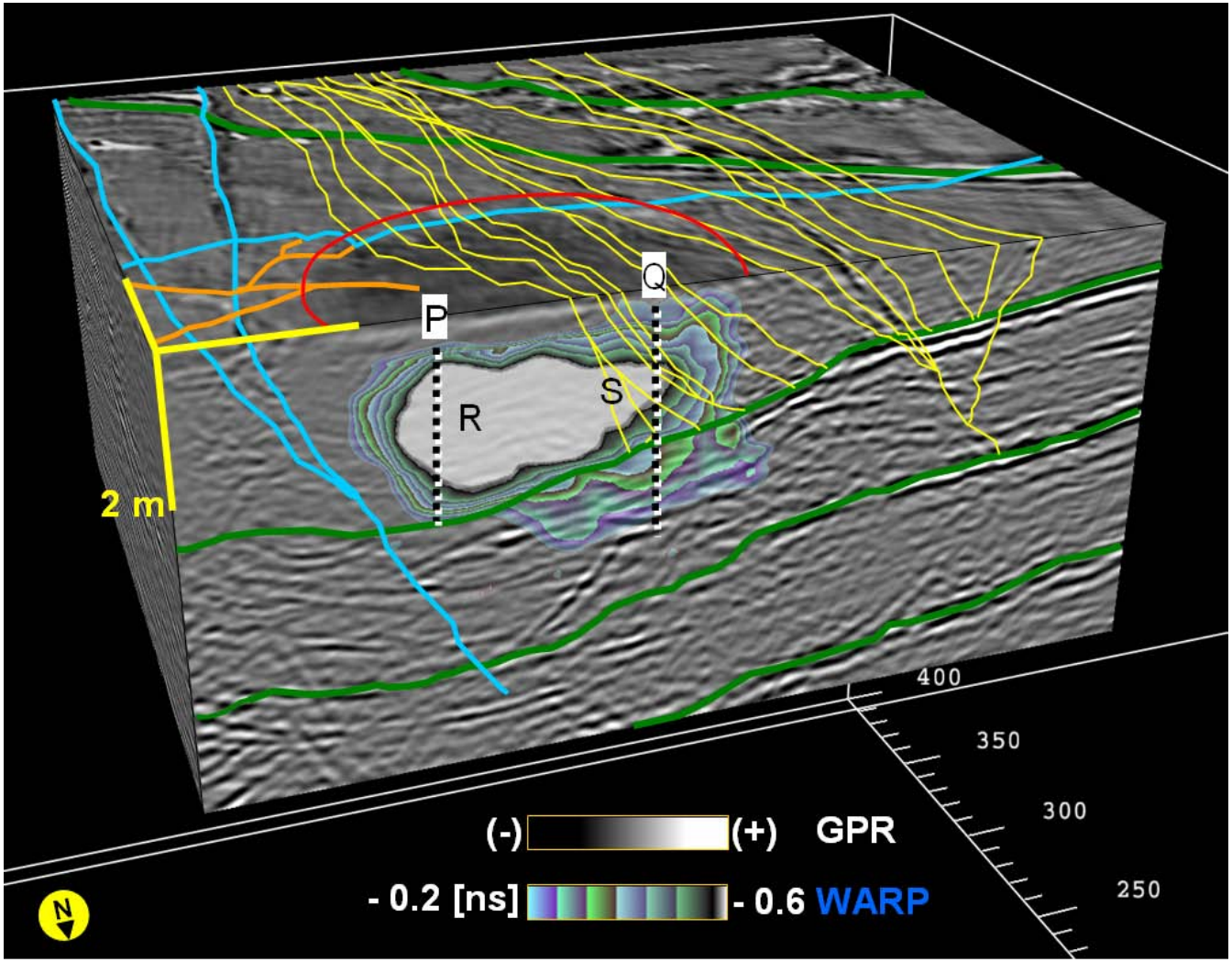

Figure 5. Semi-transparent rendering of contoured local time shift anomaly over conventional 3D GPR display. The superimposed interpretation of fractures and stratigraphy shows how the shape of the waterbulb anomaly is influenced by the steep deformation bands. The impermeable deformation bands diffuse water content changes and facilitate crossing of the stratigraphic boundary (marked green). Front face of cube displayed is part of Inline 186. Please refer to main text for explanations of labels R, S, P and Q.